

# Groundwater quality assessment for drinking and irrigation in the plains of Oran (northwestern Algeria) using GIS, water quality indices and multivariate statistical methods

## Valutazione della qualità delle acque sotterranee per uso potabile e irriguo nelle pianure di Orano (Algeria nordoccidentale) mediante GIS, indici di qualità dell'acqua e metodi statistici multivariati

Abderahim El Mehdi BELLAREDJ<sup>a</sup> 

<sup>a</sup>Laboratory for Sustainable Management of Natural Resources in Arid and Semi-arid Zones, Institute of Sciences, University Center Salhi Ahmed of Naâma (Ctr Univ Naama), 45000, Naâma, Algeria email  : [bellaredj.a@cuniv-naama.dz](mailto:bellaredj.a@cuniv-naama.dz)

### ARTICLE INFO

Ricevuto/Received: 27 March 2025  
Accettato/Accepted: 23 September 2025  
Pubblicato online/Published online:  
30 September 2025

Handling Editor:  
Stefano Viaroli

### Citation:

Bellaredj, A.E.M. (2025). Groundwater quality assessment for drinking and irrigation in the plains of Oran (northwestern Algeria) using GIS, water quality indices and multivariate statistical methods.

Acque Sotterranee - Italian Journal of Groundwater, 14(3), 33 - 50  
<https://doi.org/10.7343/as-2025-878>

### Correspondence to:

Abderahim El Mehdi Bellaredj  :  
[bellaredj.a@cuniv-naama.dz](mailto:bellaredj.a@cuniv-naama.dz)

### Keywords:

GIS, PCA and HCA, PWQI, geological zoning, climate aridity, carbonates and silicates weathering, ions exchange.

### Parole chiave:

GIS, PCA e HCA, PWQI, zonazione geologica, aridità climatica, alterazione di carbonati e silicati, scambio ionico

### Abstract

*In the southern plains of Oran, the two main aquifer formations are the Mio-pliocene limestone and the Plio-quaternary conglomerates. To assess the overall quality of groundwater, and highlight the factors and mechanisms controlling its chemistry, hydrogeological and hydrochemical data is studied using GIS, multivariate statistics (Principal Component Analysis and Hierarchical cluster analysis), potable water quality indices (PWQI) and irrigation water quality parameters. The results show that the Mio-pliocene aquifers have the best groundwater, with some samples having a mineralization of < 1g/L, whereas the quality of groundwater varies in the Plio-quaternary aquifers from one location to another. The increase in groundwater concentration generally occurs from South to North, in accordance with the direction of groundwater flow towards the Sebkh of Oran. The PCA and HCA results show that groundwater is divided into two major groups. The first represents fresh to passable waters (0,5 g/L ≤ TDS ≤ 2 g/L) located predominantly in the Tessala Mountains piedmonts and around the Taфраoui-Tlelat limestone outcrops. These groundwater have a low Langelier index (LSI ≈ 0.25) and are not corrosive nor scaling. The second group represents slightly saline to highly saline groundwater (2.5 g/L ≤ TDS ≤ 5g/L). The slightly saline groundwater are mostly observed around and South of Ain Larbaa in the Plio-quaternary conglomerates. The highly saline groundwater are only observed for 6 samples and are most likely the result of contamination. The PWQI show that only 18% of groundwater is fit for human consumption; the remaining groundwater ranging from poor (21%), very poor (38%) to unsuitable (23%). The results also show that only 60% of samples are suited for irrigation. The hydrochemical results identify geological zoning, climate aridity, and to a lesser degree anthropic activities as the major factors regulating groundwater quality via the carbonates and silicates weathering and ions exchange process.*

### Riassunto

Nelle pianure meridionali di Orano, le due principali formazioni acquifere sono il calcare mio-pliocenico e i conglomerati plio-quaternari. Per valutare la qualità complessiva delle acque sotterranee e mettere in evidenza i fattori e i meccanismi che ne controllano la chimica, i dati idrogeologici e idrochimici sono stati analizzati mediante GIS, statistiche multivariate (analisi delle componenti principali e analisi gerarchica dei cluster), indici di qualità dell'acqua potabile (PWQI) e parametri di qualità dell'acqua destinata all'irrigazione. I risultati mostrano che gli acquiferi mio-pliocenici hanno le acque sotterranee di migliore qualità, con campioni aventi una mineralizzazione < 1 g/L, mentre la qualità delle falde acquifere nelle falde acquifere plio-quaternarie varia a seconda della località. L'aumento della mineralizzazione presenta un trend generale da sud a nord, in accordo con la direzione del flusso delle acque sotterranee verso la Sebkh di Orano. I risultati PCA e HCA mostrano che le acque sotterranee si suddividono in due gruppi principali. Il primo rappresenta le acque dolci o accettabili (0,5 g/L ≤ TDS ≤ 2 g/L) situate prevalentemente ai piedi dei Monti Tessala e attorno agli affioramenti calcarei di Taфраoui-Tlelat. Queste acque sotterranee hanno un basso indice di Langelier (LSI ≈ 0,25) e non risultano né corrosive né incrostanti. Il secondo gruppo rappresenta acque sotterranee da leggermente saline ad altamente saline (2,5 g/L ≤ TDS ≤ 5 g/L). Le acque sotterranee leggermente saline si osservano principalmente intorno e a sud di Ain Larbaa nei conglomerati plio-quaternari. Le acque sotterranee altamente saline sono osservate solo in 6 campioni e sono molto probabilmente il risultato di una contaminazione. Il PWQI mostra che solo il 18% delle acque sotterranee è adatto al consumo umano; le rimanenti variano da scarse (21%), molto scarse (38%) a inadatte (23%). I risultati mostrano inoltre che solo il 60% dei campioni è adatto all'irrigazione. I risultati idrochimici identificano la zonazione geologica, l'aridità climatica e, in misura minore, le attività antropiche come principali fattori che regolano la qualità delle acque sotterranee tramite i processi di alterazione dei carbonati e silicati e di scambio ionico.

## Introduction

Groundwater is an important source of freshwater worldwide. In arid and semi-arid regions however, and due to the scarcity of surface water resources, it represents the main water supply for drinking, irrigation, cattle production, fisheries and industry needs (Adimalla et al, 2018; Li and Qian, 2018; Ferchichi et al, 2018). This excessive dependence on groundwater coupled with pollution and more and more drier climate conditions, has led to overexploitation and quality deterioration of most aquifers in these regions (Bellaredj, 2020; Ray et al, 2017; Li et al, 2017; Zahedi 2017). In several coastal regions of Algeria for instance, groundwater is a reliable source of fresh water that best meets domestic, agricultural and industrial requirements (Bouderbala 2019; Achouri et al. 2024). This is the case for the southern plains of Oran (M'lela, Taffraoui and Tlelat plains), where the annual rainfall average rarely exceeds 500 mm/year. However, groundwater quality is influenced by natural processes such as rock-water interaction, climate conditions, geological zoning and anthropic activities, such as industrialization, agriculture & livestock production and urbanization (Melki et al, 2020; Vespasiano et al, 2019). Thus, groundwater use for drinking or agricultural purposes needs to be conditioned by a thorough evaluation of its suitability and quality. Multiple techniques on the evaluation of groundwater quality are found in the literature and amongst them are geo-statistics (spatial representation based on a geographic information system GIS), multivariate statistical methods and water quality indices (WQI), which can be applied to assess both drinking (potable) and irrigation water quality. These techniques facilitate the assessment of groundwater quality and its controlling factors and are widely used to assess groundwater quality (Pham and Nguyen 2024; Thomas 2023; Musaab et al. 2022; Ismail et al. 2023; Abbasnia et al, 2018). GIS offer a better visualization of the data on the ground, even at un-sampled locations, which allows a broader understanding of the spatial and spatiotemporal trends (Maleika, 2020). Multivariate statistical methods reduce the bulk data to smaller sets, allowing an easier interpretation of the data. WQ indices on the other hand, condense multiple chemical, physical and biological variables of an x-monitoring data, like the total dissolved solids (TDS), potential hydrogen (pH), total hardness (TH), ions concentrations, sodicity, corrosiveness and scaling potential, etc., into one index based on predefined water quality guidelines.

In this work, GIS geo-statistical representation, the multivariate statistical methods, principal component analysis (PCA) and the hierarchical cluster analysis (HCA) and water quality indices are combined to analyze and interpret hydrogeological and hydrochemical data in the region. The main objectives of this study are to evaluate groundwater quality, study the spatial evolution of groundwater chemistry and identify the natural and/or anthropic processes controlling groundwater quality in the southern plains of Oran.

## Materials and Methods

### Study area

The area covered in this study is part of the watershed of the great salty lake (Sebkha) of Oran and is located south of Oran city (Fig. 1). The study area, represented by the three adjacent plains, M'lela, Taffraoui and Tlelat has an average altitude of about 100m and is limited to the North, by the Sebkha of Oran, to the South, by the Tessala Mountains, to the East, by the El-Braya & Boufatis districts and to the West, by the plain of Hammam Bouhadjar-El Malah (Fig. 1).

The stratigraphy of the region determines two structural complexes: the pre-synchrone substratum and the post-nappe infill. The Triassic is formed primarily of gypsum masses, associated with multicolored clays. The Jurassic is represented by Liassic limestone, often recrystallized, which are observed around Taffraoui. In the Tessala Mountains, Cretaceous deposits, represented by marl-schist formations are the substrate for the lower Miocene units. The red continental deposits are formed from alternating conglomerates with schist fragments, Oligocene sandstones, and red marls. Below the plains, the presence of these formations is unclear. The upper Miocene is formed of marine sandstones, blue marls, tripolis-gypsum deposits and the reef limestone that mark the end of the upper Miocene transgression. These limestone are light gray, bioclastic, oolitic, and sometimes contain coarse sandstones and light gray to bluish marls and they outcrop on the northern flank of the Tessala. In the plains, these formations lose thickness in direction to the Sebkha. The Pliocene is represented by marine marls with sandstone intercalations. Marl formations often begin with detrital sandstone or sand, sometimes conglomerate. The upper Pliocene marine sandstones correspond to yellow, calcareous sandstones that are locally very fossiliferous. In the plains, the Lower Pleistocene is present in the form of continental layers of red silt, sometimes conglomerate. The middle and upper Pleistocene layers are only observed around Ain Larbaa. The Holocene formations in the plains are mainly represented by gray salty and gypsum silts (recent alluvium) in the form of terraces.

The tectonic activity is controlled by shear and collision phases. However, upon reaching the post-nappe deposits, compression is predominant (Thomas, 1985). The tectonics are expressed along the principal directions: N10-20°, N50-70°, and N140°. The southern part of the Oran plateau is a relatively calm tectonic zone, with a slight southward dip of the formations toward the Sebkha of Oran. This extension, however, is not uniform, as it can be reversed locally, creating depressions with low points, where rainwater accumulates during the wet season. This corresponds to very low-amplitude post-Pleistocene tectonic undulations, affecting the layers of this last stage (Thomas, 1985).

From a hydrogeological standpoint, the Miocene-Pliocene limestone formations (Mio-pliocene aquifers) are the most important. These aquifers have an average thickness of 200m, a fissure permeability and are easily recharged by precipitation. At depths varying between 85 to 200 m, aquifer



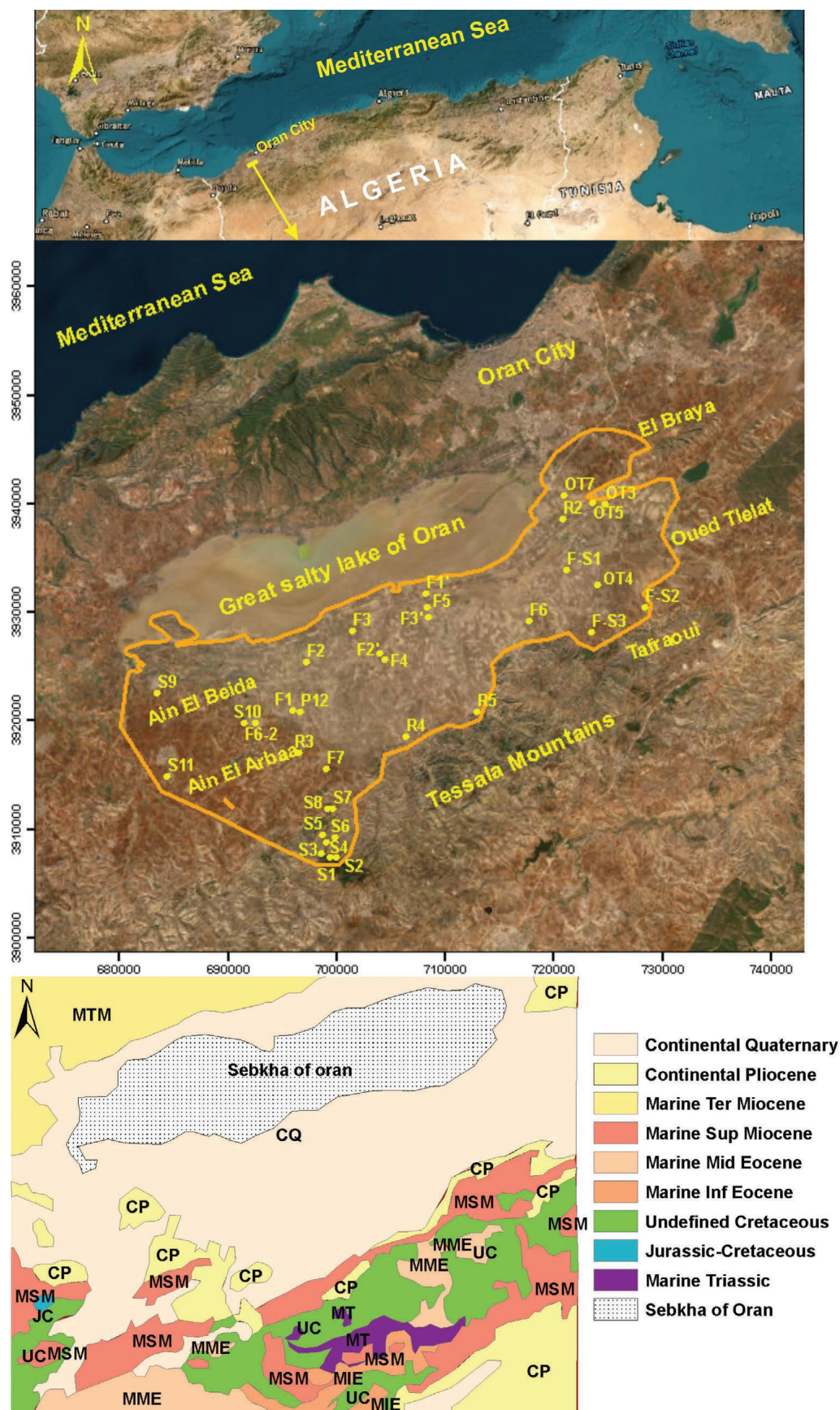


Fig. 1 - Sampling sites and geological map of the study area.

Fig. 1 - Siti di campionamento e carta geologica dell'area di studio.

levels represented by sandy and gravelly clays with calcareous pebbles are present. These Plio-Quaternary formations form fairly good aquifers and are captured by several boreholes dug by farmers (Bellaredj, 2013).

### Sampling

To evaluate groundwater quality in the region, thirty four samples were collected in October 2023. The sampling operation was targeted. Only samples currently in use (drinking and irrigation), well distributed and covering most of the study area were retained. All water samples were collected in polypropylene (PP) bottles that were rinsed several times with sample water before collection and then stored at 04 °C in ice containers to minimize exposure to light and air. All water samples were afterwards transferred to the hydrochemistry laboratory of the National Agency of hydric resources (ANRH) and analyzed the same day, based on standards from ISO for water quality analysis.

The EC was measured in-situ using a Delta Ohm conductivity meter ( $\pm 0.5\%$ ). The pH was measured in-situ using a WTW-720 pH meter ( $\pm 0.1\%$ ). For the analysis of major inorganic constituents, samples were filtered through a 0.45  $\mu\text{m}$  membrane filter. The concentrations of  $\text{HCO}_3^-$  were measured by Volumetric titration with  $\text{H}_2\text{SO}_4$  ( $\approx 1$  mg/L as  $\text{CaCO}_3$ ), those of  $\text{Cl}^-$  were estimated Argentometric titration ( $\approx 0.1$ – $1$  mg/L). The concentrations of  $\text{SO}_4^{2-}$  and  $\text{NO}_3^-$  were assessed with a UV-visible PERKIN-ELMER-lambda 25 ( $\approx 1$  mg/L and  $\approx 0.1$  mg/L respectively). The concentrations of  $\text{Ca}^{2+}$  and Mg were evaluated using the complexometric titration with EDTA ( $\approx 0.1$ – $1$  mg/L). The  $\text{Na}^+$  and  $\text{K}^+$  concentrations were estimated using a DIEIT CORNING-410 flame photometer ( $\approx 0.02$  ppm).

### Methods

The methodology adapted in this work can be summarized in four major steps (Fig. 2). Step one focuses on the general hydrochemical characterization of groundwater via the study of the main physical and chemical parameters (pH, TDS, TH,  $\text{Ca}^{2+}$ ,  $\text{Mg}^{2+}$ ,  $\text{Na}^+$ ,  $\text{K}^+$ ,  $\text{Cl}^-$ ,  $\text{SO}_4^{2-}$ ,  $\text{HCO}_3^-$  &  $\text{NO}_3^-$ ) and the identification of the main water facies using Piper diagram. Step two focuses on the study of the spatial evolution of groundwater chemistry throughout the study area to highlight the effects of geology (zonation) and anthropic activities on the overall salinity of groundwater. This was done combining punctual data (measured points) and geo-statistical methods using the GIS program ArcGIS, version 10.5. In step three, the statistical multivariate methods Principal Component Analysis (PCA) and Hierarchical Cluster Analysis (HCA) were used to classify groundwater in distinct categories (from saline waters to fresh water) based on the similarity/dissimilarity of groundwater with respect to groundwater proprieties, geology, anthropic activities and climate conditions. This was done using the software XLStat, version 2016. In Step four, the suitability of groundwater for human consumption and irrigation was assessed based on the Potable Water Quality Index (PWQI) to Principal Component

Analysis (PCA) and Hierarchical Cluster Analysis (HCA) were assess groundwater for drinking and the Electrical Conductivity (EC), Exchangeable Sodium Percentage (ESP), Permeability Index (PI) and Kelly index (KI) to evaluate groundwater fitness for irrigation.

### Geostatistics

Geo-statistics was used to study the spatial variations of groundwater quality at un-sampled locations. The study of spatial variations was done using the deterministic method based on Inverse Distance Weighting (IDW) interpolation. This technique estimates unknown values based on the distance between sampled and un-sampled locations (Chabuk et al. 2020; Mukherjee & Singh, 2021). The GIS Program ArcGIS was used for the geo-statistical analysis based on the IDW interpolation to construct spatial variation maps of EC, TH, Langelier Scaling Index (LSI), major cations and anions.

### Multivariate statistics

#### a) Principal components analysis

The PCA is a simple mathematical reduction of the quantity of data without exaggerated assumptions. The goal is to find the first principal component C1 (the one for which the variance of the individuals is maximum) and subsequently, a second component C2 that still has the maximum variance, but also has zero correlation with C1 (orthogonal to C1). The search for axes continues for the p axes, whose representativeness shares are increasingly weak, as p increases. This allows, an easier description of the information, with a considerably reduced number of variables, compared to the original set (Davies and Fearn, 2004).

The PCA is widely used in studies dealing with groundwater because it not only highlights interrelationships among multiple chemical parameters, but also reduces large datasets into smaller ones (Guenouche et al., 2024; Taşan et al., 2022).

#### b) Hierarchical cluster analysis

The HCA method consists of progressively aggregating individuals according to their resemblance measured using a similarity or dissimilarity index. It requires the definition of a measure of similarity or distance between the objects to be classified (samples) and a criterion for aggregating the classes. Initially, there is a partition into n classes, each class being composed of a single object (the finest partition). The algorithm then begins to gather the pairs of individuals that are most similar, then to progressively aggregate the other individuals or groups of individuals, until all the individuals form a single group.

HCA produces a binary classification tree called a Dendrogram, identifying at what point the different clusters are grouped. In this study, the HCA was conducted based on Ward's method (Ward & Hook, 1963).

### Groundwater quality assessment

#### a) Potable water quality index (PWQI)

The PWQI evaluates the suitability of a given water for



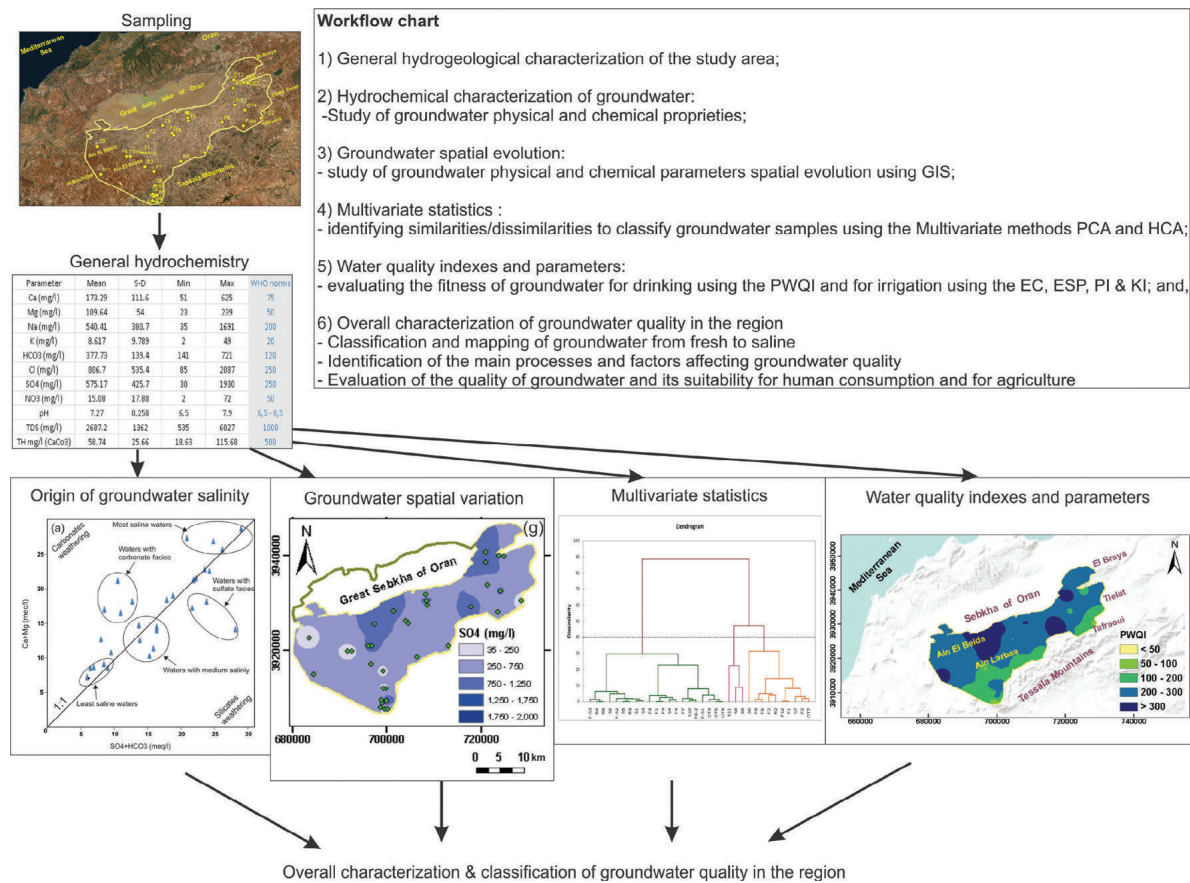


Fig. 2 - Workflow chart of the study methodology.  
Fig. 2 - Diagramma di flusso della metodologia di studio.

drinking, based on a set of selected physical and chemical parameters, which are weighted and studied in comparison to a standard set of data (Diongue et al., 2022). In this study, 10 parameters were used to calculate the PWQI, namely:  $\text{Cl}^-$ ,  $\text{HCO}_3^-$ ,  $\text{NO}_3^-$ ,  $\text{SO}_4^{2-}$ ,  $\text{Ca}^{2+}$ ,  $\text{Mg}^{2+}$ ,  $\text{Na}^+$ ,  $\text{K}^+$ , TDS and pH. The TDS and  $\text{Cl}^-$  were assigned a maximum weight of 5 due to their important impact on water quality (Wagh et al., 2019).  $\text{Na}^+$  and  $\text{Ca}^{2+}$  were assigned respective weights of 4 and 3, because of their major role in regulating water quality.  $\text{HCO}_3^-$ ,  $\text{NO}_3^-$ ,  $\text{SO}_4^{2-}$ ,  $\text{Mg}^{2+}$ ,  $\text{K}^+$  and the pH, were assigned weights between 1 and 2, in accordance with their influence on the quality of water (Gnanachandrasamy et al., 2020). The

Tab. 1 - Parameters and formulas for the PWQI.

Tab. 1 - Parametri e formule per il calcolo del PWQI.

Parameters	Formulas
The relative weight of parameters ( $W_{ri}$ )	$W_{ri} = \frac{w_i}{\sum_{i=1}^n w_i}$
The quality rating scale ( $q_i$ )	$q_i = \frac{C_i \cdot 100}{S_i}$
The water quality sub-index ( $WQSI_i$ )	$WQSI_i = W_{ri} \cdot q_i$
The Potable water quality index (PWQI)	$PWQI = \sum WQSI_i$

computational formulas and the interpretive water quality classes of the PWQI are given in Tables 1 and 2.

With:  
 $n$ : number of parameters,  
 $w_i$ : assigned weight,  
 $C_i$ : concentration of each parameter,  
 $S_i$ : standard value of each parameter.

Tab. 2 - Water class based on PWQI values (Aly et al., 2015).

Tab. 2 - Classi di qualità dell'acqua in base ai valori di PWQI (Aly et al., 2015).

PWQI	Water class
< 50	Excellent
50 - 100	Passable
100 - 200	Poor
200 - 300	Very poor
> 300	Unsuitable

b) Groundwater adaptability to irrigation

The parameters used to evaluate groundwater fitness for irrigation are the ESP, the EC and the PI and KI indexes. The equations for all parameters are given in Table 3.

Tab. 3 - Irrigation water quality parameters.

Tab. 3 - Parametri di qualità per l'acqua destinata all'irrigazione.

Parameters	Formulas	Class	Water quality
EC (dS/m)		< 0.7 0.7- 3 3 – 6 6-14 >14	Non saline Slightly saline Moderately saline Saline Highly saline
ESP	$ESP = \frac{100(-0.0126 + 0.01475 \cdot SAR)}{1 + (-0.0126 + 0.01475 \cdot SAR)}$	<6 6–10 10–15 >15	Non sodic Slightly sodic Moderately sodic Highly sodic
PI	$\frac{(Na + \sqrt{HCO_3})100}{(Ca + Mg + Na)}$	>75 25-75 <25	Good Suitable Unsuitable
KI	$\frac{Na}{(Ca + Mg)}$	<1 >1	Suitable Unsuitable

## Results and discussion

### General Hydrochemistry

In this section, the chemical and physical parameters of groundwater are studied in comparison to the WHO standards to evaluate their compliance with international norms. The hydrochemical analysis results are presented in table 4 alongside the World Health Organization (WHO) standards (Bellaredj, 2025).

The pH varies from slightly acidic (6.5) in some samples to slightly basic (7.9) for most samples (average pH  $\approx$  7.3) and is within limits of the WHO norms. TDS values vary from 0.5 g/L to 6 g/L with an average of 2.7 g/L. Only 5 samples have TDS values in accordance with the WHO for drinking water (1 g/L). TH values range from 17 mg/L to 116 mg/L of CaCO<sub>3</sub> with an average concentration of 59 mg/L and show that most samples belong to the fresh water class (TH < 75 mg/L CaCO<sub>3</sub>), with only 7 samples exceeding this limit. All samples have TH values significantly smaller than the WHO limit (500 mg/L of CaCO<sub>3</sub>).

Variations in TDS and TH values can be the result of water-rock interaction, arid climate conditions and anthropic activities. High TDS and TH values are typical of shallow, unconfined, alluvial aquifers, which are: rich in clay and evaporate minerals, more sensitive to climate change (low rainfall/high temperatures) and vulnerable to pollution. In these types of aquifers, the dominant natural geochemical processes are dissolution, precipitation, ion exchange and silicates weathering (Razi et al., 2024).

Low TDS and TH values are usually associated with non-polluted karst aquifers or deep confined aquifers, which are predominantly sandstone and/or limestone. In these types of aquifers, the dominant natural process is dissolution and to a lesser degree silicates weathering (Li et al., 2025).

With respect to ions concentrations, most samples have ion concentrations exceeding the WHO limits, especially for Cl<sup>-</sup>, SO<sub>4</sub><sup>2-</sup>, Na<sup>+</sup> and Ca<sup>2+</sup>. The concentrations of NO<sub>3</sub><sup>-</sup> and K<sup>+</sup>

Tab. 4 - Hydrochemical analysis of groundwater.

Tab. 4 - Analisi idrochimica delle acque sotterranee.

Stat mg/L	Mean	S-D	Min	Max	WHO norms
Ca <sup>2+</sup>	173.29	111.6	51	625	75
Mg <sup>2+</sup>	109.64	54	23	239	50
Na <sup>+</sup>	540.41	380.7	35	1691	200
K <sup>+</sup>	8.617	9.789	2	49	20
HCO <sub>3</sub> <sup>-</sup>	377.73	139.4	141	721	120
Cl <sup>-</sup>	806.70	535.4	85	2087	250
SO <sub>4</sub> <sup>2+</sup>	575.17	425.7	30	1930	250
NO <sub>3</sub> <sup>-</sup>	15.08	17.88	2	72	50
pH	7.27	0.258	6.5	7.9	6,5 - 8,5
TDS	2687.2	1362	535	6027	1000
TH	58.74	25.66	18.63	115.68	500

are overall in accordance with WHO guidelines (20 mg/ and 45 mg/L respectively).

These groundwater trends are commonly observed in Algeria due to climate change, abundance of clay & evaporites in most alluvial aquifers and excessive groundwater extraction (Ouarekh et al., 2020; Guenouche et al., 2024; Lalaoui et al., 2024; Benmarce et al., 2023).

Based on the molar ratio Na<sup>+</sup>/Cl<sup>-</sup>, 9 samples have a ratio equal or inferior to 0.86, suggesting seawater intrusion; 11 samples have a ratio around 1, inferring halite dissolution; 14 samples have a ratio superior to 1, probably due to silicates weathering and/or anthropogenic contamination (Liu et al., 2024).

According to the molar ration Ca<sup>2+</sup> / SO<sub>4</sub><sup>2-</sup>, 60% of samples show an excess of sulfates over calcium. This suggests that gypsum dissolution is not the only source of sulfate in groundwater; other probable sources are evaporation (concentration of dissolved sulfate), the dissolution of other sulfate minerals and anthropogenic sources (Dogramaci et al., 2025).

Regarding the molar ratio  $\text{Ca}^{2+}/\text{Mg}^{2+}$ , 23 samples have a ratio  $\leq 1$ ; 7 samples have a ratio between 1 & 2 and only 4 samples have a ratio  $> 2$ . This suggests that dolomite dissolution is dominant process ( $\text{Ca}^{2+}/\text{Mg}^{2+} \leq 1$ ), followed by calcite dissolution ( $2 \geq \text{Ca}^{2+}/\text{Mg}^{2+} > 1$ ) and silicates weathering ( $\text{Ca}^{2+}/\text{Mg}^{2+} > 2$ ) (Juárez et al., 2023).

Regarding  $\text{NO}_3^-$ , the high concentrations observed around Ain Larbaa and Ain Beida are probably due to anthropic activity (wastewaters, agricultural runoff) in these regions. Nitrogen compounds found in groundwater are usually due to agricultural activity (fertilizers, manure leaching) or to the microbial degradation of organic matter (Craswell, 2021).

From a chemical facies stand point, the Piper diagram shows that two main water facies are present. The chloride and sulfate waters rich in calcium and magnesium and the chloride and sulfate waters rich in sodium and potassium (Fig. 3).

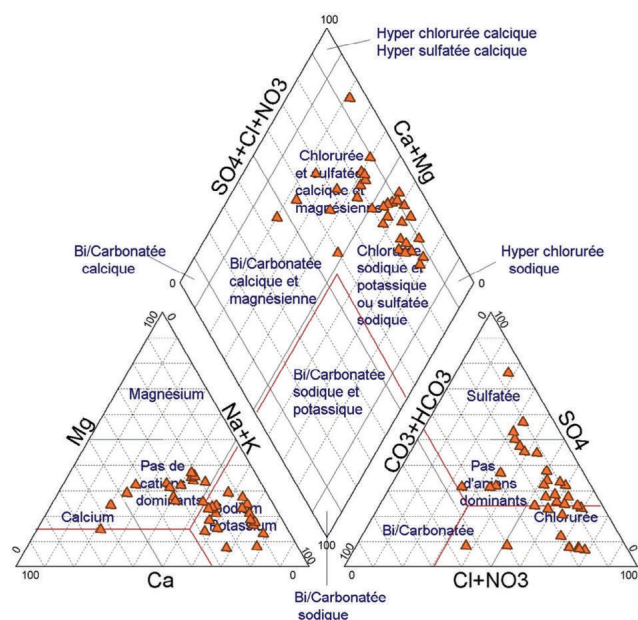


Fig. 3 - Groundwater representation on Piper's diagram.

Fig. 3 - Rappresentazione delle acque sotterranee sul diagramma di Piper.

### Spatial variation of groundwater parameters

In this section, the spatial distribution of groundwater chemistry is evaluated through the mapping of 8 parameters, namely: TDS, TH, Langelier Index,  $\text{Ca}^{2+}$ ,  $\text{Na}^+$ ,  $\text{Cl}^-$ ,  $\text{SO}_4^{2-}$  and  $\text{NO}_3^-$ , using the IDW interpolation.

#### IDW interpolation

IDW is a deterministic method that assigns weights based on distance. It relies on a fixed mathematical formula to

determine the influence of known points on unknown points, based on their distance. There are multiple other interpolation techniques, such as, natural neighbor, spline, topo to Raster, kriging, etc. Kriging for instance, is an advanced geostatistical procedure that generates an estimated surface from a scattered set of points with X variable. However, unlike other interpolation methods, kriging relies on a deep understanding of the spatial behavior of the represented X variable before generating the output surface. In comparison to kriging, the IDW doesn't require specific assumptions about the underlying data distribution (spatial correlation).

In this work, the IDW interpolation was preferred to dismiss assumptions about groundwater parameters being spatially correlated. The validity of this choice was reinforced by cross-validation of both IDW & kriging interpolations.

Cross-validation involves temporarily removing a data point, predicting its value using the remaining data, and then comparing the predicted value to the actual value. This process is repeated for all data points to assess the overall accuracy of the interpolation method.

Then, the RMSE (Root Mean Squared Error) is used to evaluate both methods performance by providing a measure of how well predictions match the actual values (Table 5).

### Groundwater parameters

The spatial variability of TDS, depicted in Figure 4, demonstrates significant spatial heterogeneity, with notable geologic zonation and anisotropic behavior. Lower TDS values, characteristic of non-saline groundwater, are primarily located near the piedmont zones of the Tessala Mountains, in the southern portion of the study area. These zones correspond to recharge areas where hydraulic gradients and relatively unaltered lithologies limit solute accumulation. In contrast, elevated TDS concentrations are spatially clustered near the Sebkhia in the north. This pattern aligns with regional hydrodynamic anisotropy, where both surface and subsurface flow vectors converge towards the salty lake, enhancing solute transport and progressive mineralization along the flow path (Fig. 5). The increase in salinity is consistent with advective transport combined with evaporative concentration, leading to TDS values exceeding 4 g/L in downgradient zones.

The spatial distribution of TH does not exhibit a direct correlation with the principal flow direction. High TH values show strong spatial association with specific geologic domains, particularly near Ain Larebaa and in the eastern zones around Taфраoui and Tlelat. These areas coincide with the carbonate-rich stratigraphic units, where water-matrix interactions favor calcite and dolomite dissolution, resulting

Tab. 5 - Comparison between the RMSE values of the Kriging model and the IDW model.

Tab. 5 - Confronto tra i valori di RMSE ottenuti dal Kriging e dall'IDW.

RMSE / Interpolation	Parameter (mg/L)						
	TDS	TH	LSI	$\text{Ca}^{2+}$	$\text{Na}^+$	$\text{Cl}^-$	$\text{SO}_4^{2-}$
IDW	1252.47	27.08	0.25	111.8	313.86	435.47	421.56
kriging	1267.05	24.75	0.26	120.77	411.33	507.41	414.44



in elevated concentrations of  $\text{Ca}^{2+}$  and  $\text{Mg}^{2+}$ . The presence of scaling conditions, as confirmed by  $\text{LSI} > 0.3$  and  $\text{Ca}^{2+} > 200 \text{ mg/L}$ , further supports the role of lithological zonation in defining the spatial distribution of hardness. However, the

$\text{Mg}^{2+}/\text{Ca}^{2+}$  molar ratio, which exceeds 1 for most locations, suggests inputs from non-geologic sources, such as, marine aerosols and leaching of carbonate fertilizers and construction materials containing  $\text{CaO}$  and  $\text{MgO}$  (Lebrato et al., 2020).

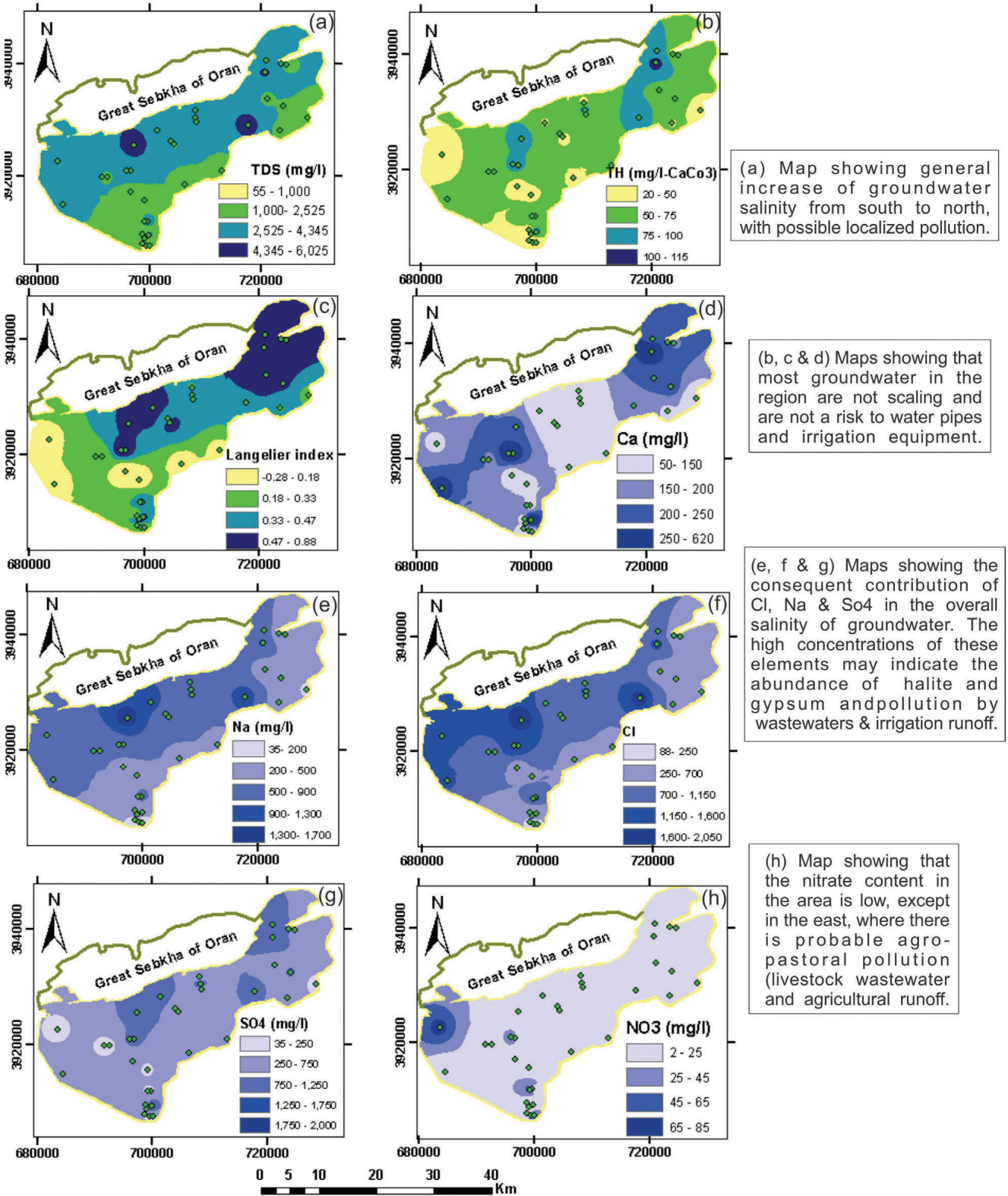


Fig. 4 - Spatial variation of groundwater parameters.

Fig. 4 - Variazione spaziale dei parametri delle acque sotterranee.



The analysis of  $\text{Cl}^-$ ,  $\text{SO}_4^{2-}$ , and  $\text{Na}^+$  maps reveals a spatial distribution highly correlated with that of TDS, underlining their strong geochemical covariance and contribution to the overall groundwater mineralization. These ions show a clear zonation tied to the occurrence of evaporitic formations (halite, gypsum), commonly found in the study area, suggesting preferential flow pathways that enhance solute migration. The spatial pattern of nitrate ( $\text{NO}_3^-$ ) shows generally low values, indicating a limited nitrification potential under natural conditions.

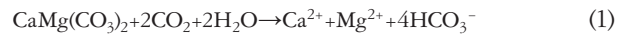
However, localized anomalies in the western part of the study area exceed the WHO threshold of 45 mg/L and suggest probable groundwater contamination by wastewaters and agricultural runoff.

### Acquisition of groundwater salinity

In this section, the probable factors and processes (natural and anthropic) controlling groundwater quality are discussed based on multiple hydrochemical formulas, scatter plots and diagrams.

On Figure 6a (Data & Tyagi diagram, 1996), most samples lie along the 1:1 line. This suggests contributions from both carbonate and silicate weathering (Manimaran et al., 2025).

Figure 6c ( $\text{HCO}_3^-$  vs  $\text{Ca}^{2+}$ ) shows that most samples fall either along or above the 1:1 line. This infers an excess of calcium over bicarbonates that could be from the dissolution of other minerals like dolomite or silicate weathering (Lechhab et al., 2024). The dissolution of dolomite and calcite are given in reactions (1&2).



The abundance of clay material and the harsh climate conditions in the region favor silicates weathering and can considerably increase the concentrations of sodium and bicarbonates in groundwater as illustrated by reactions (3&4).

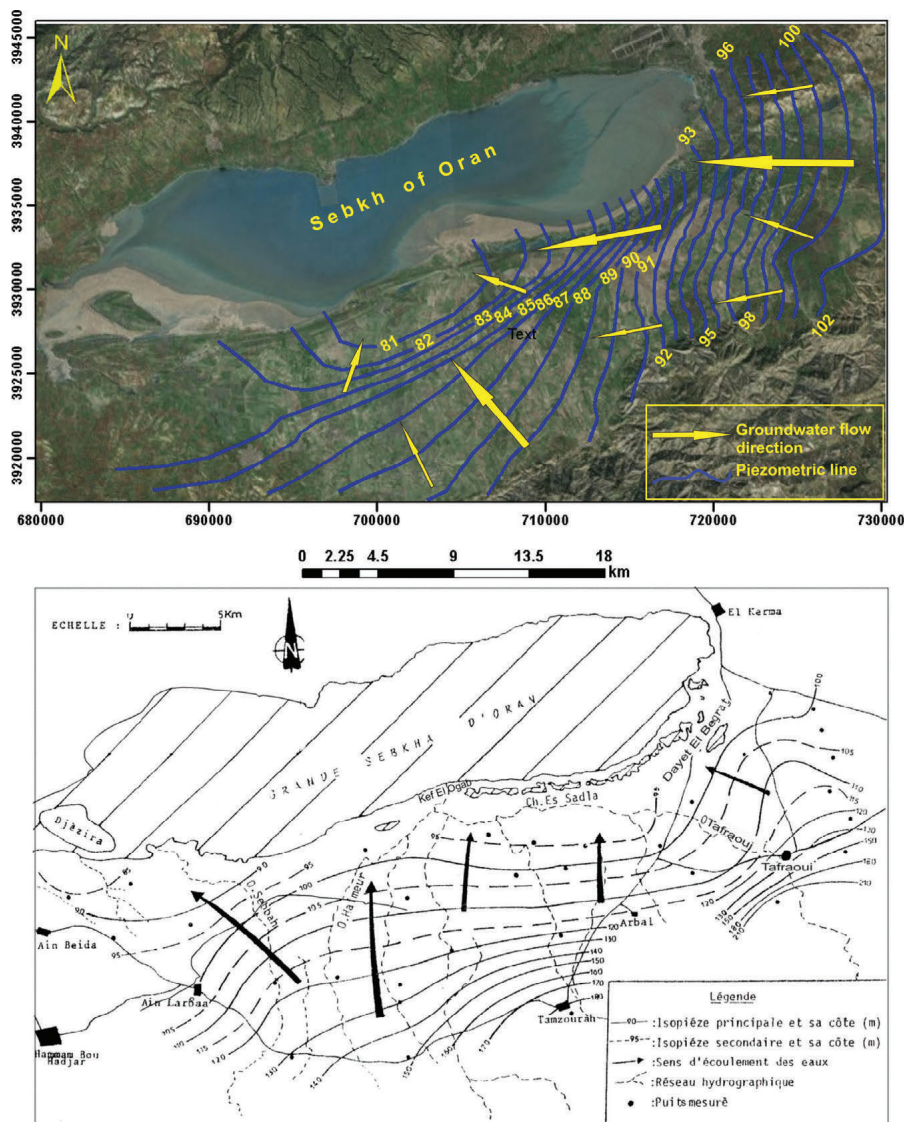
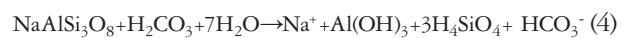
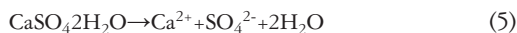


Fig. 5 - Piezometric maps of the study area; top: March 2018 & bottom: March 1986 (Hassani, 1987).

Fig. 5 - Carte piezometriche dell'area di studio; in alto: marzo 2018, in basso: marzo 1986 (Hassani, 1987).

In Figure 6b ( $\text{Ca}^{2+}$  vs  $\text{SO}_4^{2-}$ ), most samples fall below the 1:1 line. This implies an excess of  $\text{SO}_4^{2-}$  over  $\text{Ca}^{2+}$ . When the data points cluster around the 1:1 line, calcium and sulfate are released in roughly equal proportions, which is typically due to gypsum (anhydrite) dissolution (Drouiche et al., 2021).



When the data points cluster above the 1:1 line, calcium is in excess (more calcium than sulfate). This usually means the dissolution of carbonates and/or cation exchange processes, where calcium is released from the rocks material. When the data points cluster under the 1:1 line like in this case, there is an excess of sulfate over calcium. This might suggest the presence of other sulfate sources, such as oxidation of sulfide minerals or anthropic inputs (Cheng et al., 2021). The sulfate excess in the study area is probably the result of agricultural

practices, such as the use of industrial fertilizers and/or animal manure, which can lead to sulfate contamination of groundwater through leaching and infiltration (Torres-Martínez et al., 2022).

In Figure 6d ( $\text{Na}^+$  vs  $\text{Cl}^-$ ), most samples are plotted under the 1:1 line. When the data points cluster around the 1:1 line, sodium and chloride primarily come from the dissolution of halite (Kaur et al., 2019). When the  $\text{Na}^+/\text{Cl}^-$  ratio is greater than 1, this suggests that sodium is being released from the weathering of silicate minerals (Barzegar et al.; 2018). When the  $\text{Na}^+/\text{Cl}^-$  ratio is smaller than 1, like in the present case, (excess of  $\text{Cl}^-$  over  $\text{Na}^+$ ), it could be the result of multiple factors, such as, the presence of ion exchange processes and contamination by chemical fertilizers and wastewater (Kessasra et al., 2021; Dey et al., 2024).

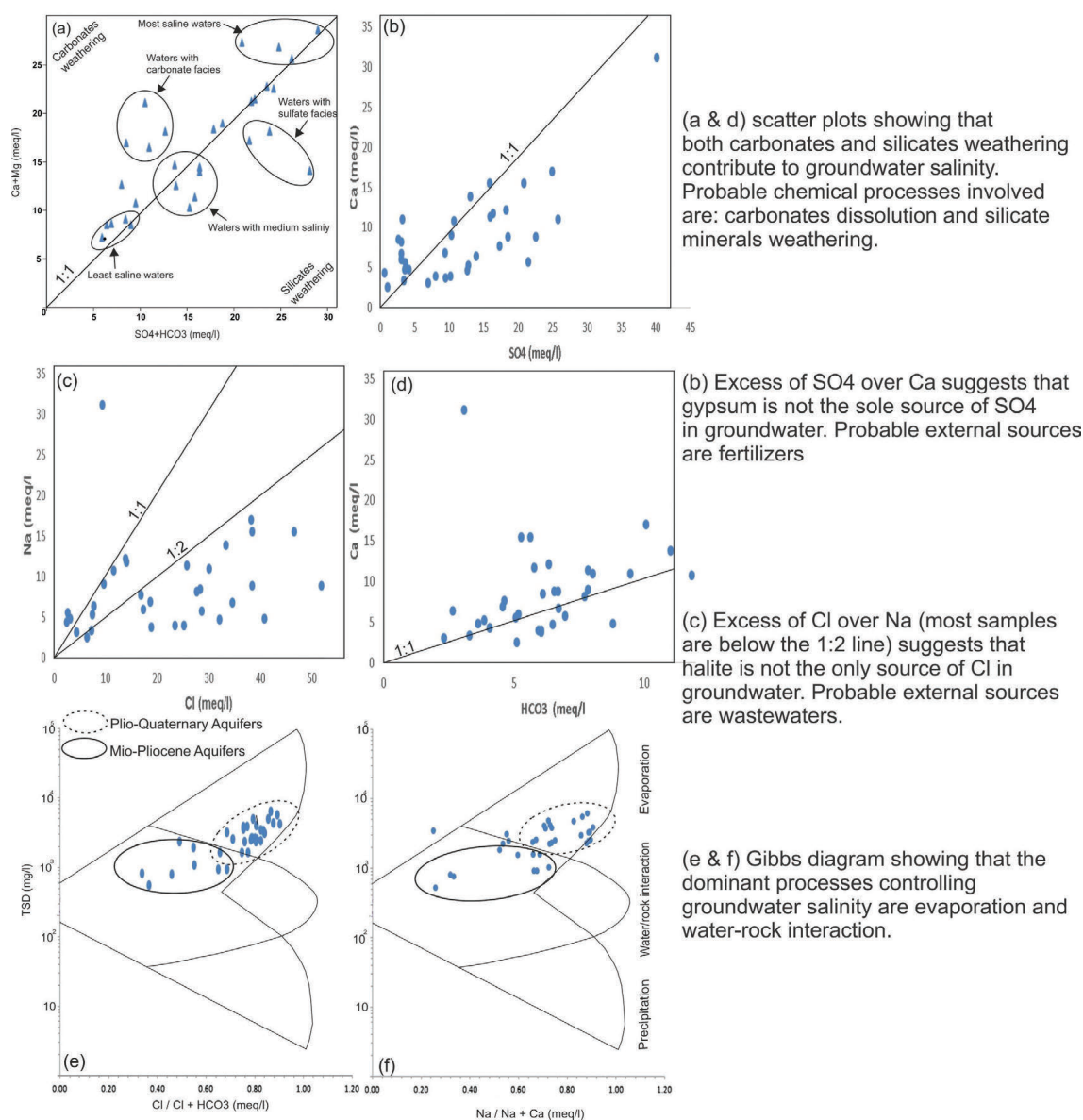


Fig. 6 - Scatter plots of hydrochemical parameters (a, b, c & d) and Gibbs diagram (e & f).

Fig. 6 - Grafici a dispersione dei parametri idrochimici (a, b, c & d) e diagrammi di Gibbs (e & f).

From the Gibbs diagram (Fig. 6 e&f), all samples fall within the areas of predominance, either of evaporation or of water/rock interaction.

The impact of climate change on groundwater in the region is evident (Fig. 7).

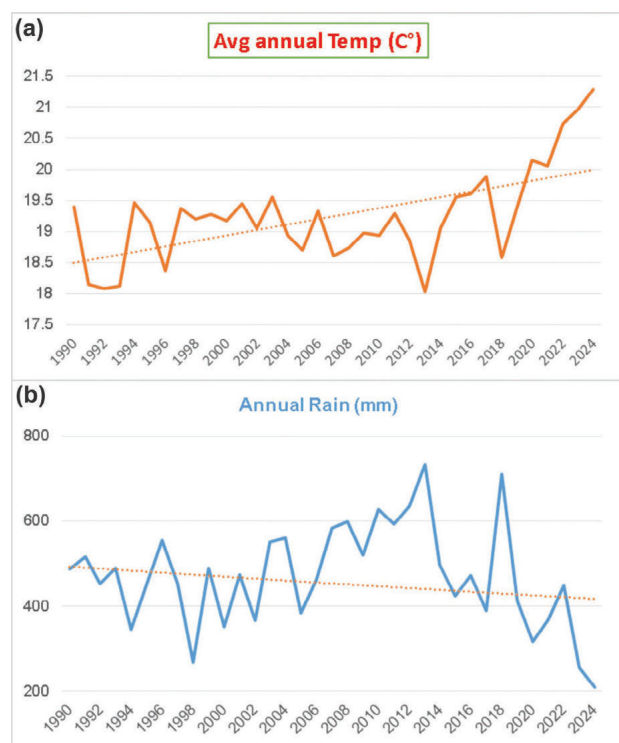


Fig. 7 - Temporal evolution of T (°C) and P (mm/y) from 1990 to 2024.

Fig. 7 - Monitoraggio delle Temperature (°C) e Piogge (mm/anno) dal 1990 al 2024.

Temperature trends from 1990 to 2024 show a clear upward pattern, with an increase of approximately 1 to 1.5°C between the early 1990s and the late 2010s. In contrast, precipitation levels have declined over the same period, with an estimated decrease of about 50 to 100 mm per year. These changes reduce surface water availability and place greater stress on groundwater resources. They also hinder aquifer recharge and increase groundwater evaporation, contributing to the overall degradation of groundwater quality and quantity.

Tab. 6 - Correlation matrix (Pearson).

Tab. 6 - Matrice di correlazione (Pearson).

Variables	Ca <sup>2+</sup>	Mg <sup>2+</sup>	Na <sup>+</sup>	K <sup>+</sup>	HCO <sub>3</sub> <sup>-</sup>	Cl <sup>-</sup>	SO <sub>4</sub> <sup>2-</sup>	NO <sub>3</sub> <sup>-</sup>	pH	TDS
Ca <sup>2+</sup>	1									
Mg <sup>2+</sup>	0.256	1								
Na <sup>+</sup>	0.196	0.640	1							
K <sup>+</sup>	0.097	-0.275	0.154	1						
HCO <sub>3</sub> <sup>-</sup>	0.196	0.431	0.536	0.404	1					
Cl <sup>-</sup>	0.239	0.687	0.933	0.189	0.548	1				
SO <sub>4</sub> <sup>2-</sup>	0.750	0.534	0.468	-0.196	0.106	0.337	1			
NO <sub>3</sub> <sup>-</sup>	-0.126	-0.194	-0.097	0.273	-0.177	0.049	-0.379	1		
pH	-0.374	0.072	-0.018	-0.614	-0.393	-0.159	0.080	-0.168	1	
TDS	0.503	0.777	0.913	0.089	0.540	0.893	0.696	-0.168	-0.115	1

## Statistical analysis

In this subsection, the Pearson correlation is used to highlight the highest and lowest correlations amongst the different physical and chemical parameters and their contribution to the overall salinity of groundwater. The PCA & HCA are used to identify the major tendencies (components & clusters) and classify groundwater based on samples similarities/dissimilarities. Data was standardized before applying PCA and HCA to prevent variables with larger magnitudes from disproportionately influencing the results.

## Pearson correlation

Based on Pearson's correlation coefficient (Table 6), the strong positive correlations ( $r > 0.7$ ) are found between: Cl<sup>-</sup> & Na<sup>+</sup> (0.933), TDS & Na<sup>+</sup> (0.913), TDS & Cl<sup>-</sup> (0.893), TDS & Mg<sup>2+</sup> (0.777), TDS & SO<sub>4</sub><sup>2-</sup> & Ca<sup>2+</sup> (0.750). High positive correlations between TDS and Na<sup>+</sup>, Cl<sup>-</sup>, Mg<sup>2+</sup> indicate that these ions are major contributors to groundwater salinity. The strong correlations suggest that as the concentration of these ions increases, the TDS level also increases, and vice versa (Mohit & Suprita, 2022).

A high correlation between Cl<sup>-</sup> & Na<sup>+</sup> typically indicates salinization, often due to halite dissolution, wastewater or agricultural runoff (Hussain et al 2024). A high correlation between SO<sub>4</sub><sup>2-</sup> & Ca<sup>2+</sup> usually infers gypsum (anhydrite) dissolution (Zhang et al., 2017). These correlations are in accordance with the results with the results discussed in § Acquisition of groundwater salinity.

## Multivariate statistics

### a) PCA

The criteria used to retain the principal components were the Kaiser's rule and the scree plot. Only components with eigenvalues > 1 (before the elbow of the scree plot) are considered significant (Table 7 & Fig. 8).

From Figure 9a1, TDS, Mg<sup>2+</sup>, Cl<sup>-</sup>, Na<sup>+</sup> and SO<sub>4</sub><sup>2-</sup> contribute more than 80% to C1, with all variables positively correlated with C1, except for potassium and nitrate ions. For C2, K<sup>+</sup> and NO<sub>3</sub><sup>-</sup> and the pH, account for more than 74%, with K<sup>+</sup>, HCO<sub>3</sub><sup>-</sup>, Ca<sup>2+</sup>, Na<sup>+</sup>, Cl<sup>-</sup> and NO<sub>3</sub><sup>-</sup> positively correlated and SO<sub>4</sub><sup>2-</sup> and Mg<sup>2+</sup> negatively correlated with C2.



Tab. 7 - Significance of PCA components by eigenvalues and variability.

Tab. 7 - Significatività delle componenti della PCA in base agli autovalori e alla variabilità.

	F1	F2	F3	F4	F5	F6	F7	F8	F9	F10
Eigenvalue	4.416	2.118	1.405	0.939	0.525	0.301	0.187	0.096	0.011	0.003
Variability (%)	44.161	21.180	14.045	9.387	5.249	3.008	1.869	0.962	0.108	0.031

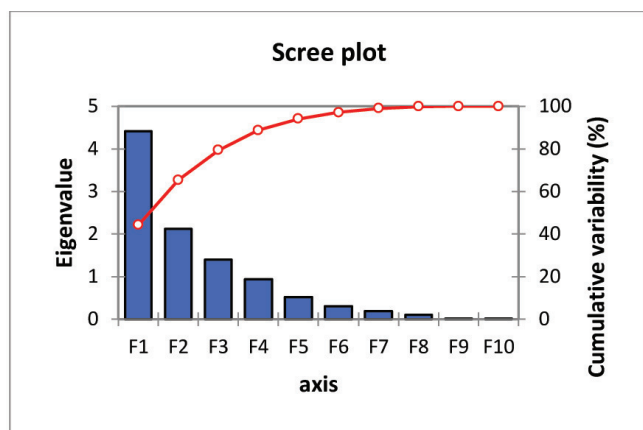


Fig. 8 - Scree plot result for the PCA.

Fig. 8 - Scree plot dei risultati della PCA.

C1 seems to indicate the general direction of salinity increase/decrease, whereas C2 appears to show the probable factors (natural or anthropic) controlling said salinity. From Figure 9a2, the more observations are positively correlated with C1&C2 the more groundwater is saline (and vice versa), probably due to halite & calcite dissolution, silicates weathering & pollution by wastewaters (high  $\text{HCO}_3^-$  and  $\text{NO}_3^-$  content & excess of  $\text{Cl}^-$  over  $\text{Na}^+$  and  $\text{Ca}^{2+}$  over  $\text{Mg}^{2+}$ ). However, the more observations are positively correlated with C1 and negatively with C2 the more groundwater is saline (and vice versa), but more likely due to dissolution of gypsum and dolomite, ion exchange and probable pollution by agricultural runoff (excess of  $\text{SO}_4^{2-}$  over  $\text{Ca}^{2+}$  and  $\text{Mg}^{2+}$  over  $\text{Ca}^{2+}$ ).

#### b) HCA

Based on the HCA results (figure 9b), the dendrogram was cut at the dissimilarity level 40, which coincides with the most abrupt changes in the dendrogram distances. The final partition contains 3 clusters, The first cluster (far left) is composed of 21 observations, the second cluster, directly to the right, is composed of 3 observations and the third cluster is composed of 10 observations. Clusters 1 & 3 regroup

groundwater mainly affected by geological zonation and evaporation. Fresh to slightly saline waters in cluster 1 are mainly located on the Tessala piedmonts in the south and on the limestone outcrops in south-east around Tafroui. Saline waters in cluster 3 are mainly observed in the center and in direction of the Sebkha of Oran. Cluster 2 regroups groundwater which seems to be polluted (high  $\text{NO}_3^-$  and  $\text{K}^+$  concentrations) by agricultural activity.

#### c) Samples subdivision

Combining the information from the PCA & HCA (Figure 9), geological zonation and the spatial variation of groundwater parameters (Figure 10), samples were subdivided into two distinct groups (Table 8).

##### - Group 01

All samples in this group are negatively correlated with the F1 axis and represent the fresh to passable waters ( $\text{TDS} \leq 2 \text{ g/L}$ ). However, these waters become, more saline when moving from the Tessala piedmonts and limestone outcrops in the South and South-East, to more sandy formations in the North. This geological zonation is accompanied by multiple facies shifts from sodium chloride waters at borehole S2 ( $\text{TDS} = 0.8 \text{ g/L}$ ) then sodium bicarbonate waters at borehole S1 ( $\text{TDS} = 0.6 \text{ g/L}$ ), to then sodium sulfate waters at borehole OT3 ( $\text{TDS} = 1.8 \text{ g/L}$ ), to finally sodium chloride waters at borehole OT4 ( $\text{TDS} = 2.2 \text{ g/L}$ ). Groundwater salinity in this group seems to be derived mainly from natural processes (dissolution of carbonates, silicates weathering, and ion exchange).

Group 1 represents neutral waters, with no corrosive or scaling risks ( $\text{LSI} \approx 0.25$ ). This group is subdivided into two Sub groups. The first sub group contains waters of excellent quality ( $\text{TDS} \approx 0.8 \text{ g/L}$ ), which are perfectly suited for drinking. The second sub group represents waters of lower quality, which are still passable for drinking water and fitted for irrigation.

##### - Group 02

Group 2 contains three subgroups, ranging from slightly saline to highly saline groundwater. The first and second subgroup includes 15 samples, with an average mineralization

Tab. 8 - Classification of groundwater based on statistical results.

Tab. 8 - Classificazione delle acque sotterranee in base ai risultati statistici.

	Group 1		Group 2		
Parameter average	Sub-G 1 (5 samples)	Sub-G 2 (8 samples)	Sub-G 1 (8 samples)	Sub-G 2 (7 samples)	Sub-G 3 (6 samples)
TDS (g/L)	0.8	2	2.5	3.5	4.8
TH mg/L ( $\text{CaCO}_3$ )	25	55	50	75	95
Langelier Index	0.1	0.4	0.32	0.44	0.56

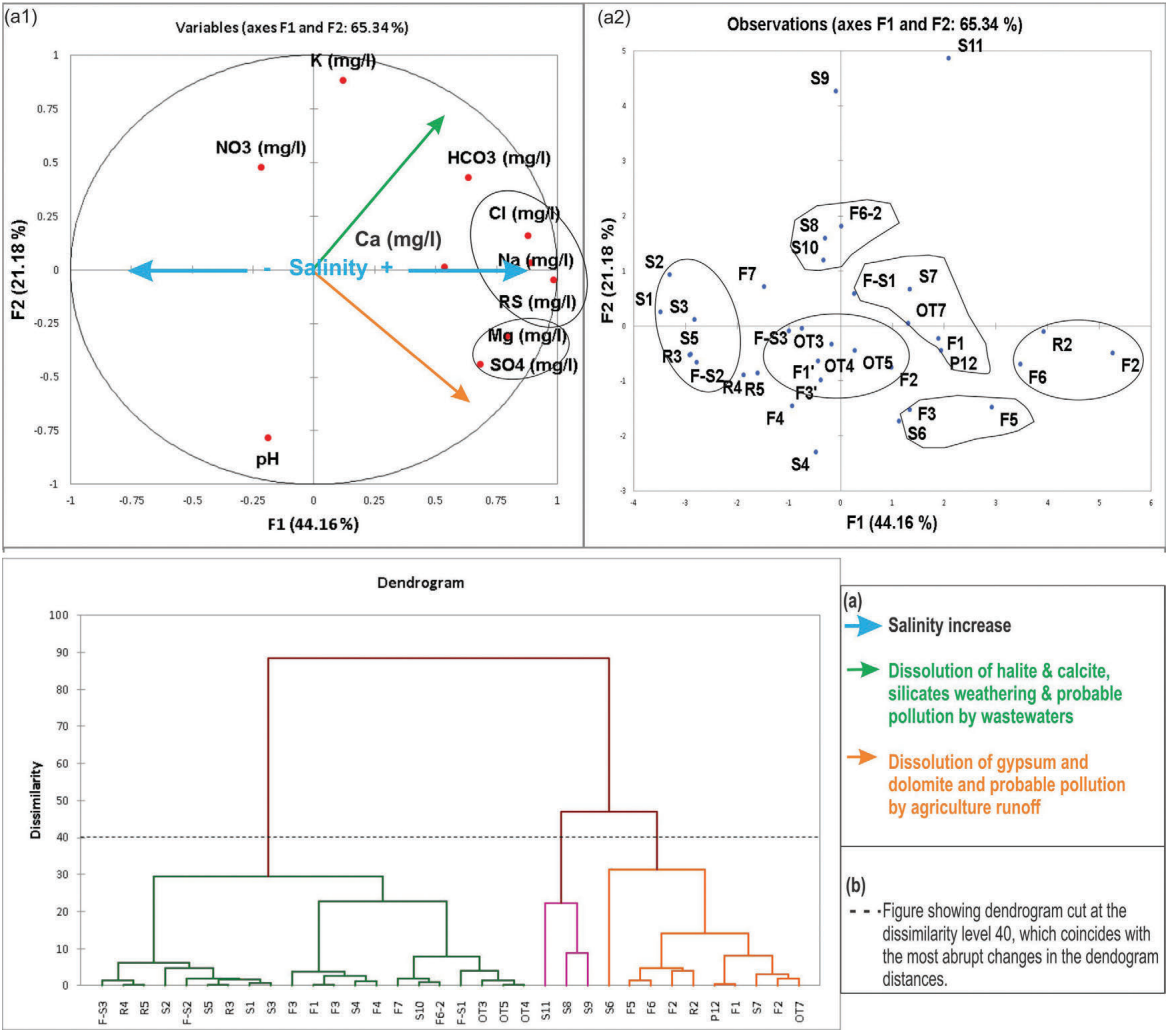


Fig. 9 - Statistical analysis results - PCA: (a1) variables & (a2) observations / HCA: (b) dendrogram.  
Fig. 9 - Risultati delle analisi statistiche – PCA: (a1) variabili & (a2) osservazioni / HCA: (b) dendrogramma.

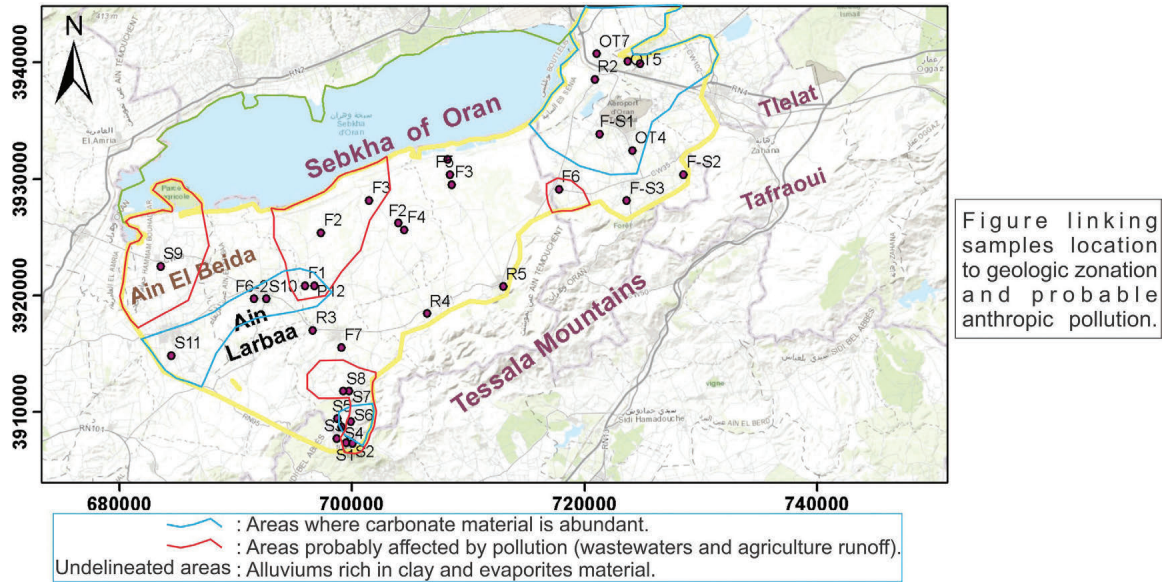


Fig. 10 - Samples location with respect to geological zonation.  
Fig. 10 - Ubicazione dei campioni in relazione alla geologia.

of 2.5-3.5 g/L. These samples are mostly found around Ain Larbaa, where the deepest Plio-quaternary levels are located (90 to 130 m of carbonate conglomerates). These waters are unfit for drinking but can be used for tolerant crops. Groundwater in subgroups 1&2 seems to be interacting with alluviums rich in carbonates, clays and evaporates material, where process such as dissolution of halite & gypsum, silicates weathering and ion exchange are dominant. The third subgroup contains 6 samples and represents the saline waters (TDS > 4.5 g/L). These waters are not only unfit for human consumption but also for irrigation. Groundwater excessive salinity for this subgroup cannot be solely explained by natural factor (water-rock interaction and evaporation), but is probably also derived from anthropic sources (wastewaters and agricultural runoff).

### Groundwater suitability for drinking and irrigation

In this final subsection, groundwater is assessed for human consumption based on the PWQI and for irrigation, based on the EC, ESP, PI & KI.

#### Potable water quality index (PWQI)

Table 9 regroups the data used to calculate the PWQI of groundwater in the study area. 10 parameters were chosen and weighted based on their impact on the quality of drinking water and the PWQI was estimated for all samples based on the WHO standard for 2022.

Tab. 9 - Groundwater data for the PWQI.

Tab. 9 - Analisi idrochimica delle acque sotterranee.

Variables	WHO (2022)	Weight (wi)	Relative weight (Wri)
Ca <sup>2+</sup>	75	3	0.111
Mg <sup>2+</sup>	50	2	0.074
Na <sup>+</sup>	200	4	0.148
K <sup>+</sup>	20	1	0.037
HCO <sub>3</sub> <sup>-</sup>	120	1	0.037
Cl <sup>-</sup>	250	5	0.185
SO <sub>4</sub> <sup>2-</sup>	250	2	0.074
NO <sub>3</sub> <sup>-</sup>	50	2	0.074
TDS	1000	5	0.185
Ph	6,5 - 8,5	2	0.074

The data in table 10 shows that only 18% of groundwater in the study area is fit for human consumption. The remaining waters range from poor (21%), very poor (38%) to unsuitable (23%). Figure 11 shows that groundwater severely deteriorates towards the north, following the general direction of water flow. This confirms that the acquisition of salinity is gradual in the direction of the Sebkh of Oran. The only groundwater fit for human consumption are found at the Tessala Mountains piedmonts, at the limestone outcrops of the Mio-pliocene aquifers around Tlelat-Taфраoui and in the vicinity of Ain Labraa in the deep Plio-quaternary conglomerate aquifer levels. These trends confirm that geological zoning, climate,

Tab. 10 - Groundwater quality based on PWQI.

Tab. 10 - Qualità delle acque sotterranee classificata in base al PWQI.

PWQI	Samples	Water Quality
< 50	1	Excellent
50 - 100	5	Passable
100 - 200	7	Poor
200 - 300	13	Very poor
> 300	8	Unsuitable

and to a lesser degree anthropic activities play a major role in conditioning groundwater quality in the region.

While a PWQI ≤ 100 generally signifies excellent to passable water quality, it doesn't guarantee potability. Potable water, needs to meet specific standards that are not included in the PWQI, such as bacterial & viral contaminants and heavy metals. Poor water quality, reflected by a PWQI > 100, is either due to natural processes or anthropic activities. In polluted environments, contaminated water can cause outbreaks of cholera, dysentery, Typhoid fever, and hepatitis A, impacting morbidity and mortality rates. High nitrate levels for instance can cause methemoglobinaemia (blue baby syndrome) in infants, while excessive fluoride can lead to dental and skeletal fluorosis (Jamshidi et al., 2021)

#### Irrigation water quality

Based on the information in Table 11, only 60% of samples are suited for irrigation overall. Out of the 60%, only 25% are adapted for most crops.

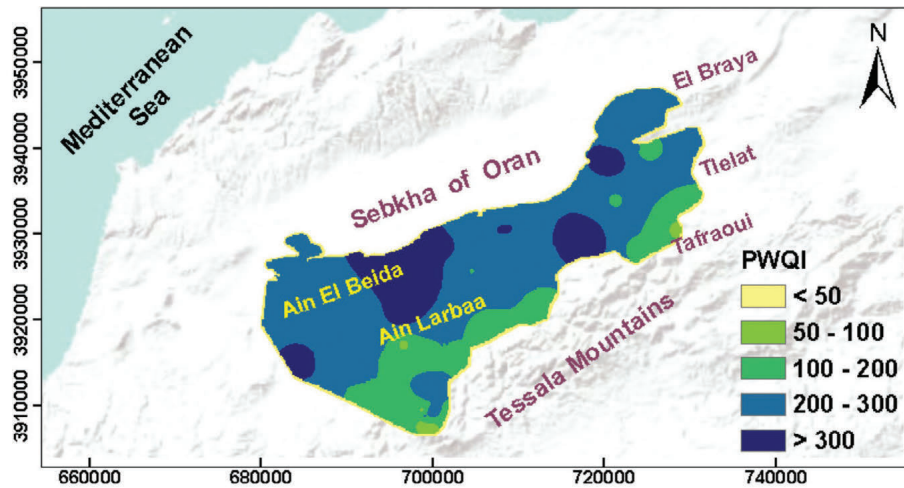
The remaining 40% of groundwater range from passable to unsuitable for irrigation. Passable waters represent close to 30% and can be used for tolerant cultures. The remaining groundwater are unfit for irrigation. Toxicity in irrigation waters is mainly tied to boron, chloride and sodium stresses. In addition to the roots, plants can also uptake considerable amounts of Na<sup>+</sup> and Cl<sup>-</sup> through the leaves during sprinkler irrigation, especially in arid regions. High concentrations of sodium in the soil are strongly harmful to crop development because they disrupt the functioning of roots and infiltrate

Tab. 11 - Groundwater fitness for irrigation.

Tab. 11 - Idoneità delle acque sotterranee all'irrigazione.

Parameters	Samples	Class	Water quality
EC (dS/m)	2	< 0.7	Non saline
	18	0.7- 3	Slightly saline
	13	3 - 6	Moderately saline
	1	6-14	Saline
	-	>14	Highly saline
ESP	15	<6	Non sodic
	8	6-10	Slightly sodic
	9	10-15	Moderately sodic
	3	>15	Highly sodic
PI	5	>75	>75
	29	25-75	25-75
	-	<25	<25
KI	16	<1	Suitable
	18	>1	Unsuitable





Map showing the severe deterioration of groundwater towards the north (PWQI > 100) in direction of the Sebkh of Oran. Groundwater fit for human consumption are only found at the Tessaia Mountains piedmonts, around Tlalat-Tafraroui and in the vicinity of Ain Larbaa.

Fig. 11 - Spatial variation of the PWQI.

Fig. 11 - Variazione spaziale del PWQI.

the aerial part of the plant causing generalized cellular intoxication (Chele et al. 2021). Based on table 12, the majority of groundwater in the region 72% is harmful to sensitive to moderately sensitive crops, and should only be used for tolerant crops.

### Results implication on groundwater management & sustainability

This study highlights that most groundwater in the region is of poor quality, especially with respect to drinking water and irrigation water for sensitive to moderately sensitive crops. The only exceptions worth mentioning are the areas where the aquifer levels are predominantly limestone/sandstone with low clay and evaporate minerals (north of Tafraroui-Tlalat, around Ain Larbaa and in the Tessaia piedmonts). These results are unfortunately superposed to the negative effects of climate change, which has led to an increase in temperatures and a significant decrease in rainfall, over the past 50 years. The findings in this work reinforce the decisions undertaken by Algerian authorities to accelerate the construction of new sea water desalination plants and the mega projects of surface water transfer from the eastern dams to the western dams of

the country to compensate for the lack of precipitation. These efforts, although colossal (there are already five desalination plants in Oran: Arzew, Bousfer, Ain Turck, Macta, and the last one in Cap Blanc, which was commissioned in February 2025), are still insufficient to guarantee an adequate supply of quality water to the city of nearly 2 million inhabitants.

### Conclusion

The hydrochemical characterization of groundwater in the southern plains of Oran shows that the dominant facies are chloride and sulfate waters rich in sodium and calcium due to the predominance of  $\text{Cl}^-$ ,  $\text{SO}_4^{2-}$ ,  $\text{Na}^+$  and  $\text{Ca}^{2+}$  ions in groundwater.

The results show that the quality of groundwater varies significantly, depending on the geology of the aquifers exploited. To the east (Tafraroui-Tlalat area) and South (Tessaia Mountains piedmonts) the Mio-pliocene aquifers have groundwater of good quality. In the center and west of the study area, the quality of groundwater in the Plio-quaternary aquifers varies from one location to another. However, and based on geo-statistical results (IDW using GIS), the increase in groundwater concentration in the region seems to

Tab. 12 - Classification of groundwater based on statistical results.

Tab. 12 - Classificazione delle acque sotterranee in base ai risultati statistici.

Tolerance levels	$\text{Cl}^-$ (mg/L)	$\text{Na}^+$ (mg/L)	Crops	N° of samples	
Sensitive	<178	<114	Almond, apricot, citrus, plum	4	3
Moderately sensitive	178–355	114–229	Capsicum, grape, potato, tomato	6	6
Moderately tolerant	355–710	229–458	Barley, cucumber, sweetcorn	7	7
Tolerant	>710	>458	Cauliflower, cotton, safflower, sesame, sorghum, sunflower	17	18

\* Credit: adapted from Bauder et al. 2014.

generally occur from the South to North, in accordance with the direction of groundwater flow, i.e., from the southern and southern eastern limit of the study area ( $\text{TDS} < 1\text{g/L}$ ), towards the Sebkhah of Oran ( $\text{TDS} > 5\text{g/L}$ ).

The application of multivariate statistical methods ACP and HCA showed that groundwater in the region can be subdivided into two major groups. The first group represents fresh to passable waters ( $0.5\text{ g/L} \leq \text{TDS} \leq 2\text{ g/L}$ ). These waters are mainly located in the Tessala piedmonts and Tafraroui-Tlelat limestone outcrops. Groundwater in group 1 are neutral waters ( $\text{LSI} \approx 0.25$ ) and do not pose corrosive or scaling risks to either the potable water network, nor irrigation equipment. The second group represents slightly saline to highly saline groundwater. The slightly saline groundwater ( $2.5\text{ g/L} \leq \text{TDS} \leq 3.5\text{ g/L}$ ) are mostly observed around and south of Ain Larbaa, due to abundance of carbonate-conglomerates in the Plio-quadernary aquifers, at depth between 90 and 130m. Regarding highly saline groundwater ( $\text{TDS} > 5\text{g/L}$ ), they are only observed for 6 samples and are probably the result of punctual pollution (most likely septic fosses and/or stagnant waters in boreholes due to rare utilization).

The water quality indices (PWQI) show that only 18% of groundwater in the study area is fit for human consumption, with the remaining waters ranging from poor (21%), very poor (38%) to unsuitable (23%). The spatial distribution of the PWQI shows that groundwater quality deteriorates considerably throughout its flow path, by accumulating more and more salts before reaching the Sebkhah of Oran.

The parameters for irrigation water quality (EC, ESP, PI and KI) show that only 60% of samples are suited for irrigation (only 25% are adapted for sensitive to moderately sensitive crops). The remaining 40% of groundwater range from passable to unsuitable for irrigation.

The hydrochemical characterization of groundwater shows that geological zoning, climate (low precipitation/high temperature), and to a lesser degree anthropic activities are the major factors regulating groundwater quality in the area. These factors heavily influence processes such as dissolution & precipitation of evaporites (mainly halite, gypsum and calcite), weathering of silicates and ion exchange phenomena.

#### Competing interest

The author declares no competing interests associated with this research and that the manuscript has no commercial or financial relationships that can cause any potential conflict of interest.

#### Acknowledgments

The author would like to acknowledge the University Center of Naama for providing the necessary resources and environment to conduct this research. The author also extends his gratitude to all the personnel of the National Agency of hydric resources and especially the team at the laboratory of hydrochemistry for their crucial support in facilitating the success of this work.

#### Author contributions

The manuscript was single authored. The author has read and approved the final manuscript.

#### Funding source

The author received no external funding and all research related activities were done using resources of the institution of affiliation.

#### Additional information

DOI: <https://doi.org/10.7343/as-2025-878>

Reprint and permission information are available writing to [acquessotterranee@anipapozzi.it](mailto:acquessotterranee@anipapozzi.it)

Publisher's note Associazione Acque Sotterranee remains neutral with regard to jurisdictional claims in published maps and institutional affiliations.

## REFERENCES

- Abbasnia, A., Yousefi, N., Mahvi, A. H., Nabizadeh, R., Radfard, M., Yousefi, M., & Alimohammadi, M. (2019). Evaluation of groundwater quality using water quality index and its suitability for assessing water for drinking and irrigation purposes: Case study of Sistan and Baluchistan province (Iran). *Human and Ecological Risk Assessment: An International Journal*, 25(4), 988-1005.
- Achouri, I., Djamel, N., Rachid, C., & Cherif, G. (2024). For A Sustainable Management of Potential Impacts of Global Change on Coastal Aquifers: Case Study of Coastal Aquifers in Annaba City, Algeria. *Pol. J. Environ. Stud*, 20(10), 1-1.. <https://doi.org/10.15244/pjoes/191174>
- Adimalla, N., Li, P., & Venkatayogi, S. (2018). Hydrogeochemical evaluation of groundwater quality for drinking and irrigation purposes and integrated interpretation with water quality index studies. *Environmental Processes*, 5, 363-383. <https://doi.org/10.1007/s40710-018-0297-4>
- Aly, A.A., Al-Omran, A.M. & Alharby, M.M. The water quality index and hydrochemical characterization of groundwater resources in Hafar Albatin, Saudi Arabia. *Arab J Geosci* 8, 4177–4190 (2015). <https://doi.org/10.1007/s12517-014-1463-2>
- Barzegar, R., Asghari Moghaddam, A., & Tziritis, E. (2016). Assessing the hydrogeochemistry and water quality of the Aji-Chay River, northwest of Iran. *Environmental earth sciences*, 75, 1-15. <https://doi.org/10.1007/s12665-016-6302-1>
- Bauder, T. A., Davis, J. G., & Waskom, R. M. (2014). Managing saline soils. Fact Sheet No. 0.503, Crop Series| Soil.
- Bellaredj, A. E. M. (2025). Hydrochemical analysis of groundwater in the southern plains of Oran (Northwestern Algeria).. figshare. Dataset. <https://doi.org/10.6084/m9.figshare.3007046>
- Bellaredj, A. E. M. (2013). Caractérisation des eaux souterraines de la plaine de la M'leta (Algérie, Nord-ouest) par application de méthodes statistiques multivariées et modélisation géochimique. Mémoire de Magister, Université d'Oran, 2, 143.
- Bellaredj, A. E., & Hamidi, M. (2020). Computer modelling of groundwater overexploitation: case study from the plain of Sidi Bel Abbès (northwestern Algeria). *Journal of Fundamental and Applied Sciences*, 12(1), 257-290.
- Benmarce, K., Hadji, R., Hamed, Y., Zahri, F., Zighmi, K., Hamad, A., ... & Besser, H. (2023). Hydrogeological and water quality analysis of thermal springs in the Guelma region of North-Eastern Algeria: A study using hydrochemical, statistical, and isotopic approaches. *Journal of African Earth Sciences*, 205, 105011. <https://doi.org/10.1016/j.jafrearsci.2023.105011>
- Bouderbala, A. (2019). The impact of climate change on groundwater resources in coastal aquifers: case of the alluvial aquifer of Mitidja in Algeria. *Environmental Earth Sciences*, 78(24), 698.

- Chabuk, A., Al-Madhloom, Q., Al-Maliki, A., Al-Ansari, N., Hussain, H. M., & Laue, J. (2020). Water quality assessment along Tigris River (Iraq) using water quality index (WQI) and GIS software. *Arabian Journal of Geosciences*, 13, 1-23. <https://doi.org/10.1007/s12517-020-05575-5>
- Chele, K. H., Tinte, M. M., Piater, L. A., Dubery, I. A., and Tugizimana, F. (2021). Soil salinity, a serious environmental issue and plant responses: A metabolomics perspective. *Metabolites*, 11(11), 724. <https://doi.org/10.3390/metabo11110724>
- Cheng, L., Jiang, C., Li, C., & Zheng, L. (2022). Tracing sulfate source and transformation in the groundwater of the linhuan coal mining area, huaibei coalfield, China. *International Journal of Environmental Research and Public Health*, 19(21), 14434. <https://doi.org/10.3390/ijerph192114434>
- Craswell, E. (2021). Fertilizers and nitrate pollution of surface and ground water: an increasingly pervasive global problem. *SN Applied Sciences*, 3(4), 518. <https://doi.org/10.1007/s42452-021-04521-8>
- Datta, P. S., & Tyagi, S. K. (1996). Major ion chemistry of groundwater in Delhi area: chemical weathering processes and groundwater flow regime. *Journal geological society of India*, 47(2), 179-188. <https://doi.org/10.17491/jgsi/1996/470205>
- Davies, T., & Fearn, T. (2004). Back to basics: the principles of principal component analysis. *Spectroscopy Europe*, 16(6), 20. Dey, S., Veerendra, G. T. N., Manoj, A. V. P., & Padavala, S. S. A. B. (2024). Removal of chlorides and hardness from contaminated water by using various biosorbents: A comprehensive review. *Water-Energy Nexus*, 7, 39-76. <https://doi.org/10.1016/j.wen.2024.01.003>
- Diongue, D. M., Sagnane, L., Emvoutou, H., Faye, M., Gueye, I. D., & Faye, S. (2022). Evaluation of groundwater quality in the deep maastrichtian aquifer of senegal using multivariate statistics and water quality index-based GIS. *Journal of Environmental Protection*, 13(11), 819-841. <https://doi.org/10.4236/jep.2022.1311052>
- Dogramaci, S., Wallis, I., Cook, P., & Kneeshaw, A. (2025). Hydrochemical evolution of groundwater in a semi-arid environment verified through natural tracer and geochemical modelling, northwest Australia. *Applied Geochemistry*, 183, 106337. <https://doi.org/10.1016/j.apgeochem.2025.106337>
- Drouiche, A., Zahi, F., Debieche, T. H., Lekoui, A., & Mahdid, S. (2022). Assessment of surface water quality: a case of Jijel region, North-East Algeria. *Arabian Journal of Geosciences*, 15(3), 252. <https://doi.org/10.1007/s12517-022-09458-9>
- Ferchichi, H., Ben Hamouda, M. F., Farhat, B., & Ben Mammou, A. (2018). Assessment of groundwater salinity using GIS and multivariate statistics in a coastal Mediterranean aquifer. *International journal of environmental science and technology*, 15, 2473-2492. <https://doi.org/10.1007/s13762-018-1767-y>
- Guenouche, F. Z., Mesbahi-Salhi, A., Zegait, R., Chouia, S., Kimour, M. T., & Bouslama, Z. (2024). Assessing water quality in North-East Algeria: a comprehensive study using water quality index (WQI) and PCA. *Water Practice & Technology*, 19(4), 1232-1248. <https://doi.org/10.2166/wpt.2024.073>
- Gibbs, R. J. (1970). Mechanisms controlling world water chemistry. *Science*, 170(3962), 1088-1090. <https://doi.org/10.1126/science.170.3962.1088>
- Gnanachandrasamy, G., Dushiyanthan, C., Jeyavel Rajakumar, T., & Zhou, Y. (2020). Assessment of hydrogeochemical characteristics of groundwater in the lower Vellar river basin: using Geographical Information System (GIS) and Water Quality Index (WQI). *Environment, development and sustainability*, 22, 759-789. <https://doi.org/10.1007/s10668-018-0219-7>
- Hao, Q., Xiao, Y., Chen, K., Zhu, Y., & Li, J. (2020). Comprehensive understanding of groundwater geochemistry and suitability for sustainable drinking purposes in confined aquifers of the Wuyi Region, Central North China Plain. *Water*, 12(11), 3052. <https://doi.org/10.3390/w12113052>
- Hassani, M. I. (1986). Hydrogéologie d'un Bassin Endoréique Semi-aride: Le Bassin Versant de la Grande Sebkhah d'Oran' "*Hydrogeology of a Semi-arid Endorheic Basin: The Watershed of the Great Sebkhah of Oran*" (Doctoral dissertation, Thèse de Doctorat de 3ème Cycle, Grenoble, France).
- Hussain, S., Wang, Y., Awais, M., Sajjad, M. M., Ejaz, N., Javed, U., ... & Iqbal, J. (2024). Integrated assessment of groundwater quality dynamics and Land use/Land cover changes in rapidly urbanizing semi-arid region. *Environmental Research*, 260, 119622. <https://doi.org/10.1016/j.envres.2024.119622>
- Ismail, E., Snousy, M. G., Alexakis, D. E., Gamvroula, D. E., Howard, G., El Sayed, E., ... & Abdelhalim, A. (2023). Multivariate statistical analysis and geospatial mapping for assessing groundwater quality in West El Minia District, Egypt. *Water*, 15(16), 2909. <https://doi.org/10.3390/w15162909>
- Jamshidi, A., Morovati, M., Golbini Mofrad, M. M., Panahandeh, M., Soleimani, H., & Abdolapour Alamdari, H. (2021). Water quality evaluation and non-cariogenic risk assessment of exposure to nitrate in groundwater resources of Kamyaran, Iran: spatial distribution, Monte-Carlo simulation, and sensitivity analysis. *Journal of Environmental Health Science and Engineering*, 19(1), 1171131. <https://doi.org/10.1007/s40201-021-00678-x>
- Juárez, J. E. R., Alvarado, M. A. A., Zamarron, A. S., González, O. A., Hernandez, V. H. B., Trujillo, E. O., & de Alba, Á. A. V. (2023). Chemical conditioning of drinking groundwater through Ca<sup>2+</sup>/Mg<sup>2+</sup> ratio adjust as a treatment to reduce Ca precipitation: batch assays and test bench experiments. *Journal of Water Process Engineering*, 53, 103844. <https://doi.org/10.1016/j.jwpe.2023.103844>
- Kaur, L., Rishi, M. S., Sharma, S., Sharma, B., Lata, R., & Singh, G. (2019). Hydrogeochemical characterization of groundwater in alluvial plains of river Yamuna in northern India: An insight of controlling processes. *Journal of King Saud university-science*, 31(4), 1245-1253. <https://doi.org/10.1016/j.jksus.2019.01.005>
- Kawo, N. S., & Karuppannan, S. (2018). Groundwater quality assessment using water quality index and GIS technique in Modjo River Basin, central Ethiopia. *Journal of African earth sciences*, 147, 300-311. <https://doi.org/10.1016/j.jafrearsci.2018.06.034>
- Kessasra, F., Benabes, D., Seraoui, S., Chetibi, N. E. H., Mesbah, M., Khaled-Khodja, S., & Foughalia, A. (2021). Groundwater flow and chloride transport modeling of the alluvial aquifer of lower Soummam Valley, Béjaia, North-East of Algeria. *Journal of African Earth Sciences*, 173, 104023. <https://doi.org/10.1016/j.jafrearsci.2020.104023>
- Lalaoui, M., Bouchareb, N., Bousbia, S., Rebbah, A. C., Baali, M., Belmekimah, D., & Fekraoui, R. (2024). Assessment of Water Quality for Drinking and Domestic Use from Three Sources in the Mila Region, Northeastern Algeria. *Asian Journal of Water, Environment and Pollution*, 21(6), 151-159. <https://doi.org/10.3233/AJW240082>
- Lechhab, W., Lechhab, T., Tligui, Y., Fakhil Lanjri, A., Fath Allah, R., Cacciola, F., & Salmoun, F. (2024). Assessing hydrogeochemical characteristics, pollution sources, water quality, and health risks in Northwest Moroccan springs using statistical analysis. *Sustainable Water Resources Management*, 10(5), 169. <https://doi.org/10.1007/s40899-024-01147-7>
- Lebrato, M., Garbe-Schönberg, D., Müller, M. N., Blanco-Ameijeiras, S., Feely, R. A., Lorenzoni, L., ... & Oeschlies, A. (2020). Global variability in seawater Mg: Ca and Sr: Ca ratios in the modern ocean. *Proceedings of the National Academy of Sciences*, 117(36), 22281-22292. <https://doi.org/10.1073/pnas.1918943117>
- Li, C., Fang, J., Feng, F., Yao, T., Shan, Y., & Su, W. (2025). Differential Evolution in Hydrochemical Characteristics Amongst Porous, Fissured and Karst Aquifers in China. *Hydrology*, 12(7), 175. <https://doi.org/10.3390/hydrology12070175>
- Li, R., Kuo, Y. M., Liu, W. W., Jang, C. S., Zhao, E., & Yao, L. (2018). Potential health risk assessment through ingestion and dermal contact arsenic-contaminated groundwater in Jiangnan Plain, China. *Environmental geochemistry and health*, 40, 1585-1599. <https://doi.org/10.1007/s10653-018-0073-4>



- Li, P., & Qian, H. (2018). Water resources research to support a sustainable China. *International Journal of Water Resources Development*, 34(3), 327-336. <https://doi.org/10.1080/07900627.2018.1452723>
- Li, P., Tian, R., Xue, C., & Wu, J. (2017). Progress, opportunities, and key fields for groundwater quality research under the impacts of human activities in China with a special focus on western China. *Environmental Science and Pollution Research*, 24, 13224-13234. <https://doi.org/10.1007/s11356-017-8753-7>
- Liu, Y., Li, M., Zhang, Y., Wu, X., & Zhang, C. (2024). Analysis of the hydrogeochemical characteristics and origins of groundwater in the changbai mountain region via inverse hydrogeochemical modeling and unsupervised machine learning. *Water*, 16(13), 1853. <https://doi.org/10.3390/w16131853>
- Maleika, W. (2020). Inverse distance weighting method optimization in the process of digital terrain model creation based on data collected from a multibeam echosounder. *Applied Geomatics*, 12(4), 397-407. <https://doi.org/10.1007/s12518-020-00307-6>
- Manimaran, D., Abishek, S. R., Pitchaimani, V. S., Ravindran, A. A., Soniyamary, M., & Karuppannan, S. (2025). Spatial variation and hydrogeochemical characterization of groundwater in Vallanadu region: insights from water quality index and statistical analysis. *Discover Sustainability*, 6(1), 524. <https://doi.org/10.1007/s43621-025-01381-9>
- Melki, S., Asmi, A. M. E., Sy, M. O. B., & Gueddari, M. (2020). A geochemical assessment and modeling of industrial groundwater contamination by orthophosphate and fluoride in the Gabes-North aquifer, Tunisia. *Environmental Earth Sciences*, 79(6), 135. <https://doi.org/10.1007/s12665-020-8857-0>
- Mohit, M., & Suprita, S. (2022). A Review on Correlation Between the Total Dissolved Salts (TDS) and Electrical Conductivity (EC) of Water Samples Collected From Different Area of Bhiwani City, Haryana, India. *International journal of health sciences*, 6(S6), 5431-5438. <https://doi.org/10.53730/ijhs.v6nS6.10821>
- Mukherjee, I., & Singh, U. K. (2021). Characterization of groundwater nitrate exposure using Monte Carlo and Sobol sensitivity approaches in the diverse aquifer systems of an agricultural semiarid region of Lower Ganga Basin, India. *Science of the Total Environment*, 787, 147657. <https://doi.org/10.1016/j.scitotenv.2021.147657>
- Mohammed, M. A., Szabó, N. P., & Szűcs, P. (2022). Multivariate statistical and hydrochemical approaches for evaluation of groundwater quality in north Bahri city-Sudan. *Heliyon*, 8(11). <https://doi.org/10.1016/j.heliyon.2022.e11308>
- Ouarekh, M., Bouselsal, B., Belksier, M. S., & Benaabidate, L. (2021). Water quality assessment and hydrogeochemical characterization of the Complex Terminal aquifer in Souf valley, Algeria. *Arabian Journal of Geosciences*, 14(21), 2239. <https://doi.org/10.1007/s12517-021-08498-x>
- Pham, H., Rahman, M. M., Nguyen, N. C., Le Vo, P., Le Van, T., & Ngo, H. (2017). Assessment of surface water quality using the water quality index and multivariate statistical techniques—A case study: the upper part of Dong Nai river basin, Vietnam. *Journal of water sustainability*, 7(4), 225-245.
- Pham, N. Q., & Nguyen, G. T. (2024). Evaluating groundwater quality using multivariate statistical analysis and groundwater quality index. *Civil Engineering Journal*, 10(3), 699-713. <https://doi.org/10.28991/CEJ-2024-010-03-03>
- Ray, R. K., Syed, T. H., Saha, D., Sarkar, B. C., & Patre, A. K. (2017). Assessment of village-wise groundwater draft for irrigation: a field-based study in hard-rock aquifers of central India. *Hydrogeology Journal*, 25(8), 2513-2525. <https://doi.org/10.1007/s10040-017-1625-x>
- Razi, M. H., Wilopo, W., & Putra, D. P. E. (2024). Hydrogeochemical evolution and water-rock interaction processes in the multilayer volcanic aquifer of Yogyakarta-Sleman Groundwater Basin, Indonesia. *Environmental Earth Sciences*, 83(6), 164. <https://doi.org/10.1007/s12665-024-11477-6>
- Taşan, M., Demir, Y., & Taşan, S. (2022). Groundwater quality assessment using principal component analysis and hierarchical cluster analysis in Alaçam, Turkey. *Water Supply*, 22(3), 3431-3447. <https://doi.org/10.2166/ws.2021.390>
- Thomas, G. (1985). *Géodynamique d'un bassin intramontagneux: Le bassin du bas Cheliff occidental (Algérie) durant le Mio-Plio-Quaternaire "Geodynamics of an intramontane basin: The Lower Western Cheliff Basin (Algeria) during the Mio-Plio-Quaternary"*. Pau, France: Univ. Pau et Pays de l'Adour.
- Thomas, E. O. (2023). Evaluation of groundwater quality using multivariate, parametric and non-parametric statistics, and GWQI in Ibadan, Nigeria. *Water Science*, 37(1), 117-130. <https://doi.org/10.1080/23570008.2023.2221493>
- Torres-Martínez, J. A., Mora, A., Knappett, P. S., Ornelas-Soto, N., & Mahlknecht, J. (2020). Tracking nitrate and sulfate sources in groundwater of an urbanized valley using a multi-tracer approach combined with a Bayesian isotope mixing model. *Water Research*, 182, 115962. <https://doi.org/10.1016/j.watres.2020.115962>
- Vespasiano, G., Cianflone, G., Romanazzi, A., Apollaro, C., Dominici, R., Polemio, M., & De Rosa, R. (2019). A multidisciplinary approach for sustainable management of a complex coastal plain: The case of Sibari Plain (Southern Italy). *Marine and Petroleum Geology*, 109, 740-759. <https://doi.org/10.1016/j.marpetgeo.2019.06.031>
- Wagh, V.M., Mukate, S.V., Panaskar, D.B. et al. Study of groundwater hydrochemistry and drinking suitability through Water Quality Index (WQI) modelling in Kadava river basin, India. *SN Appl. Sci.* 1, 1251 (2019). <https://doi.org/10.1007/s42452-019-1268-8>
- Ward Jr, J. H., & Hook, M. E. (1963). Application of an hierarchical grouping procedure to a problem of grouping profiles. *Educational and psychological measurement*, 23(1), 69-81.
- Zahedi, S. (2017). Modification of expected conflicts between drinking water quality index and irrigation water quality index in water quality ranking of shared extraction wells using multi criteria decision making techniques. *Ecological Indicators*, 83, 368-379. <https://doi.org/10.1016/j.ecolind.2017.08.017>
- Zhang, Q., Wang, H., Wang, Y., Yang, M., & Zhu, L. (2017). Groundwater quality assessment and pollution source apportionment in an intensely exploited region of northern China. *Environmental Science and Pollution Research*, 24, 16639-16650. <https://doi.org/10.1007/s11356-017-9114-2>